AEGC2019 Data to Discovery
Australasian Exploration Geoscience Conference
2-5 September 2019 • Perth, Western Australia
Incorporating the AIG, ASEG, PESA, and WABS

Full waveform inversion of simultaneous long-offset data

Nizar Chemingui
PGS
15375 Memorial Drive, Suite 100
Houston, TX, 77079, USA
Nizar.Chemingui@pgs.com

Alejandro A. Valenciano
PGS
15375 Memorial Drive, Suite 100
Houston, TX, 77079, USA
Alejandro.Valenciano@pgs.com

Andrew Long*
PGS
Level 4, IBM Centre, 1060 Hay Street
West Perth, WA, 6005, Australia
Andrew.Long@pgs.com

SUMMARY

The standard workflow for velocity model building (VMB) in complex regimes is an interpretive process that requires time-consuming manual intervention, and remains an error-prone process that can produce suboptimal results. We discuss an application of Full Waveform Inversion (FWI) to automate the refinement of legacy velocity models generated by conventional workflows. We demonstrate our solution on a full-azimuth (FAZ) survey acquired in the Gulf of Mexico using dual-sensor streamers and blended sources in the form of simultaneous long-offsets (SLO). The dual-sensor acquisition provides low-frequency data, while the SLO configuration enables the recording of long offsets in excess of 16 km; thereby providing a unique dataset to meet the traditional data dependencies for robust FWI stability. The long offsets and low frequencies were key to using both refractions and reflections to update the deeper parts of the velocity model. Our solution directly inverts the simultaneous data as acquired in the field, and is particularly relevant to the industry growth in blended seismic data acquisition. We also employed an FWI velocity gradient that eliminates the migration isochrones; thereby removing the reflectivity imprint from the model updates. The FWI application to the field survey successfully refined the geometry of the salt bodies, including the base salt and the intra-salt enclosures. It also improved the RTM image; particularly the salt flanks and the subsalt reflectors.

Key words: FWI, long offset, velocity model building, simultaneous shooting, seismic imaging.

INTRODUCTION

Full Waveform Inversion (FWI) is the tool of choice for building high-resolution velocity models. It involves nonlinear minimization of the misfit between the recorded and modelled seismic data while iteratively updating the subsurface model. The success of FWI depends on the seamless recovery of the short- and long-wavelength features missing in the starting velocity model.

Most FWI applications have targeted shallow water environments where the recorded refracted and diving waves enable the inversion to resolve the small-scale geologic features up to the deepest turning point (e.g. Sirgue et al., 2009; Zhou et al., 2015). Recently, there have been successful FWI applications in deep-water scenarios where refracted and diving waves are often missing due to limited far offsets in towed-streamer acquisitions. Consequently, there has been a growing demand for acquiring better data for FWI, e.g., longer offsets from ocean bottom seismic (Shen et al., 2017) and lower frequencies with a high signal-to-noise ratio (Dellinger et al., 2016). Alternatively, FWI developments have focused on better inversion solutions that can reduce the data requirements and produce deep model updates. These efforts have targeted combinations of modified gradients, robust norms for measuring the data misfit, and a priori model constraints to enable utilization of all wave modes in the data (reflections, refractions, and diving waves).

We combine an acquisition strategy that employs simultaneous shooting to record long offset data and a robust FWI solution that inverts both reflections and transmitted arrivals. Our inversion simulates the blended data as acquired in the field. Therefore, no separation of the simultaneous sources is required during data preparation.

ACQUISITION OF LONG-OFFSET AND LOW-FREQUENCY DATA

The survey used here was designed to acquire high-fold, long offset, and full-azimuth (FAZ) data in the Central and Western planning areas of the Gulf of Mexico (Long *et al*., 2014). Two streamer vessels were used, each towing 10 x 8 km dual-sensor streamers. The acquisition employed three additional source vessels in a simultaneous long-offset (SLO) configuration (Figure 1).

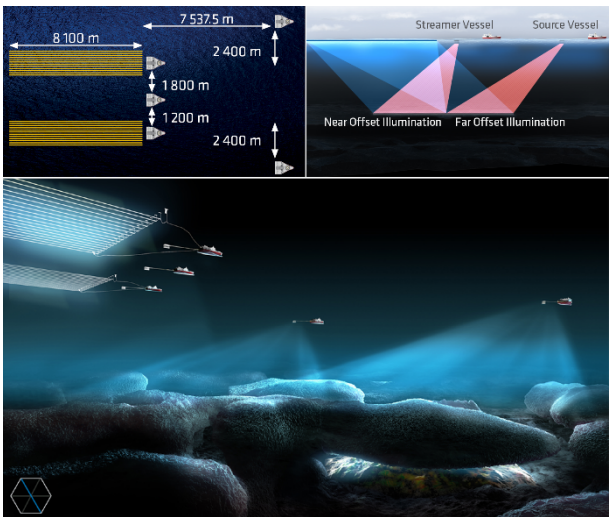

Figure 1. Five-vessel configuration (upper left and lower) employed for simultaneous long-offset shooting (upper right).

The two far sources ahead of the streamer vessels were fired simultaneously with a random delay from the near sources on the two streamer vessels, thereby providing offsets of about 16

km. The near source vessel between the streamer vessels fired independently from the others. The sailing configuration was antiparallel, and the acquisition template was repeated in three different azimuths (0, 60, and 120 degrees), ensuring full azimuth coverage of the deep targets. The dual-sensor streamers were towed at 20 m to obtain a good signal-to-noise ratio at the lower end of the frequency spectrum. As a result, the data contained low frequencies, wide azimuths, and long offsets—all beneficial for FWI. The water depth for the test area varied from 1200 m to 1400 m.

FWI ON BLENDED DATA

Our inversion algorithm uses time-domain wave propagation and a normalized form of the Born scattering kernel to compute the FWI gradient (Tarantola, 1984). We solve the two-way anisotropic wave equation using the pseudo analytic (PA) method (Ramos-Martinez et al., 2011). We use a variable-density implementation for better matching of the relative amplitudes; particularly from the water-bottom reflections and high-contrast interfaces. We implemented a robust velocity gradient derived from Inverse Scattering theory and impedance-velocity parameterization of FWI (Ramos-Martinez et al., 2016). This eliminates the migration isochrones that dominate conventional cross-correlation FWI gradients (Figure 2).

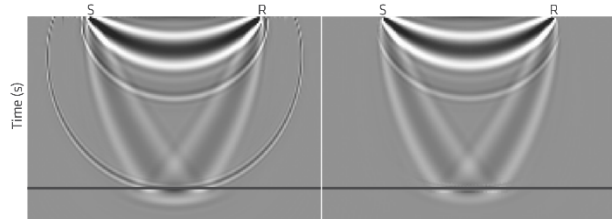

Figure 2. Sensitivity kernels for a source-receiver pair in a model with a V(z) layer over a half-space. (left) Conventional cross-correlation FWI gradient; and (right) FWI velocity gradient for long wavelength model updates. The implementation on the right eliminates the migration isochrones and removes the reflectivity footprint.

The modelling kernel for the FWI algorithm was elegantly adapted to accommodate data from simultaneous shooting; a methodology that is increasingly common in modern marine seismic surveys. Figure 3A shows a blended shot gather corresponding to both near and far sources (see Figure 1). The horizontal axis includes the 8.1 km streamer spreads and the near and far sources, with offset varying from 125 m to about 16 km. Figure 3B displays synthetic data from the near source only, while Figure 3C shows data from the blended near and far sources. The difference between panel 3B and 3C represents the long offset recordings from the far source.

APPLICATION TO SURVEY FIELD DATA

To minimize the likelihood of cycle skipping, we performed a multi-stage FWI starting with data that exhibited coherent signal in the 2-4 Hz frequency band. The initial velocity model was generated using an interpretive VMB workflow that included wavelet-shift tomography and salt interpretation following a top-down strategy.

Figure 4 compares the data fitting using the starting model (Figure 4A) and the FWI model (Figure 4B). Figure 4A shows a good match of the near source refractions, with an error smaller than half the period of the dominant frequency. After FWI the small kinematic mismatches are corrected, as well as the larger errors at later arrivals (marked by arrows pointing to refracted energy from the far source).

Figure 5 shows a comparison of the updates using only refractions (A) and a combination of refractions and reflections (B). Note that the refracted modes only produce reliable velocity updates up to 6 km depth. In contrast, our robust FWI velocity gradient is able to use the reflections to update the velocity model beyond the penetration depth of diving waves. Figure 6 shows a comparison of the RTM images from the initial (A) and the FWI (B) velocity models. The FWI velocity model improves the image of the salt boundaries (top, bottom, and flanks) as well as the sediment truncations against the salt. Similarly, the deeper reflectors display improved continuity after FWI.

Figure 7 further validates the FWI model improvements. While Figures 7A and 7B compare the RTM images before and after model updating, respectively, Figures 7C and 7D illustrate the refinement process of the velocity model by FWI. The errors in the salt interpretation (C) are corrected by FWI (D) that removes salt (blue updates) and adds salt (red updates), as needed.

CONCLUSIONS

We discussed an automated workflow for refining velocity models in complex regimes using data from simultaneous long-offset recordings and a robust FWI gradient that incorporates reflection data for deep model updating. Our inversion simulates the blended data as acquired in the field without source separation. Application to a long-offset dual-sensor survey from the Gulf of Mexico demonstrated that FWI is able to refine the sediment velocities and repair the geometry of the salt including the intra-salt enclosures. It also improved the RTM image particularly the salt flanks and the subsalt reflectors.

ACKNOWLEDGEMENTS

We thank PGS MultiClient for permission to use the field data. We also thank Jan Egil Kirkebø for assistance with the field data, and Lingyun Qiu, Dan Whitmore, and Faqi Liu for helpful discussions.

REFERENCES

Dellinger, J., Ross, A., Meaux, D., Brenders, A., Gesoff, G., Etgen, J., Naranjo, J., Openshaw, G., and Harper, M., 2016, Wolfspar, an 'FWI-friendly' ultralow-frequency marine seismic source: 86th Meeting, SEG, Dallas, Expanded Abstracts, 4891-4895.

Long, A., Campbell, S., Fishburn, S., Brandsberg-Dahl, S., Chemingui, N., and Dirks, V., 2014, No-compromise marine seismic: A full-azimuth survey design for total-wavefield velocity model building and imaging in the deep-water Gulf of Mexico: 84th Meeting, SEG, Denver, Expanded Abstracts, 52-56.

Ramos-Martinez, J., Crawley, S., Kelly, S., and Tsimelzon, B., 2011, Full-waveform inversion by pseudo-analytic extrapolation: 81st Meeting, SEG, San Antonio, Expanded Abstracts, 2684-2688.

Ramos-Martinez, J., Crawley, S., Zou, Z., Valenciano, A.A., Qiu, L. and Chemingui, N., 2016, A robust gradient for long wavelength FWI updates: 76th Meeting, EAGE, Vienna, Extended Abstracts, Th SRS2 03.

Shen, X., Ahmed, I., Brenders, A., Dellinger, J., Etgen, J., and Michell, S., 2017, Salt model building with full-waveform inversion: 87th Meeting, SEG, Anaheim, Expanded abstracts, 1507-1511.

Sirgue, L., Barkved, O.I., Van Gestel, J.P., Askim, O.J. and Kommedal, J.H., 2009, 3D waveform inversion on Valhall wide-azimuth OBC: 71st Meeting, EAGE, Amsterdam, Extended Abstracts, U038.

Tarantola, A., 1984, Inversion of seismic reflection data in the acoustic approximation: Geophysics, 49, 8, 1259-1266.

Zhou, W., Brossier, R., Operto S., and Vireux, J., 2015, Full waveform inversion of diving waves for velocity model building with impedance inversion based on scale separation: Geophysical Journal International, 202, 1535-1554.

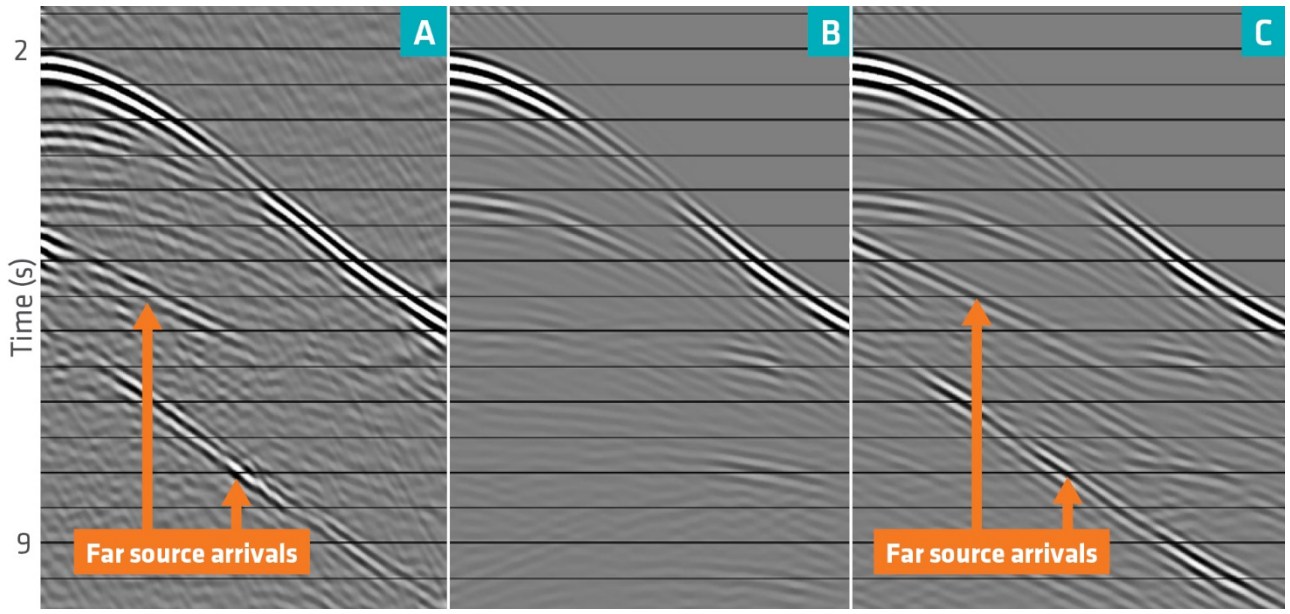

Figure 3. Shot records: (A) field data; (B) modelled data from the near source; and (C) modelled blended data from simultaneous near and far sources.

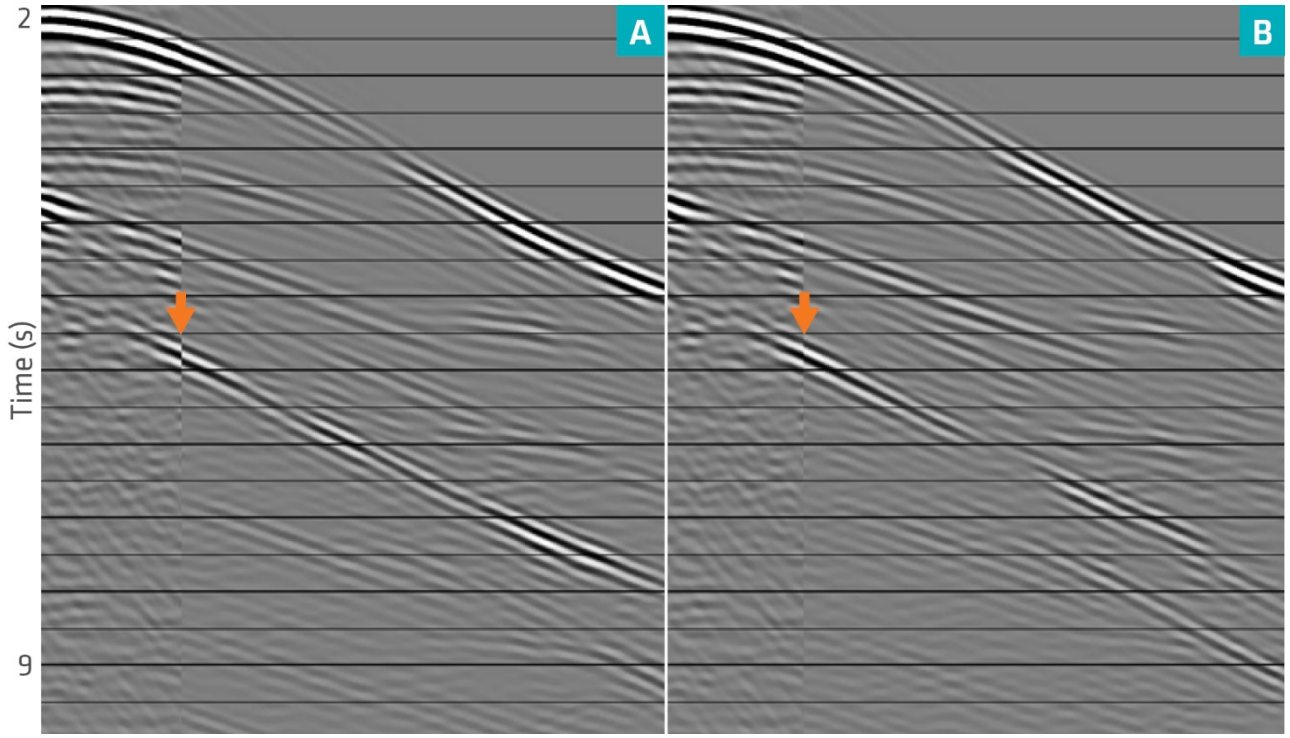

Figure 4. Comparison of field data (left of arrow) and modelled data (right of arrow). (A) Data modelled with the initial model; and (B) data modelled with FWI model. Note the improved match after FWI of the far-source events marked by the arrows.

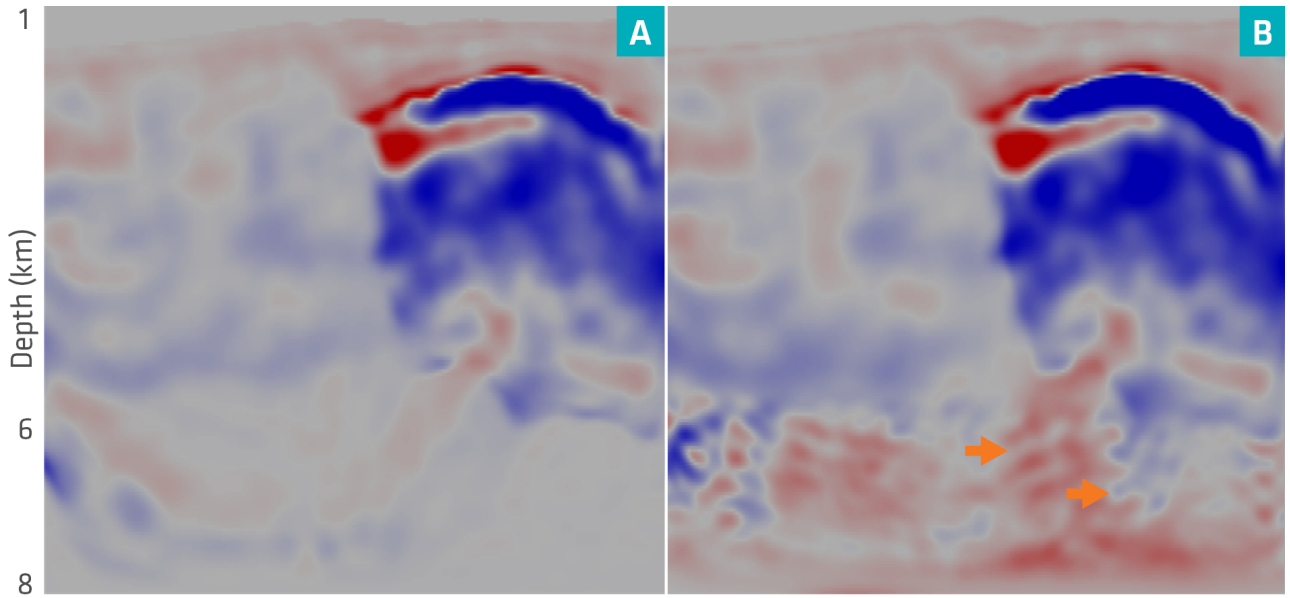

Figure 5. FWI updates comparison: using only refractions (A), vs. using combined refractions and reflections (B). Reflections can update the long wavelength components of the velocity model beyond the penetration depth of diving waves (orange arrows).

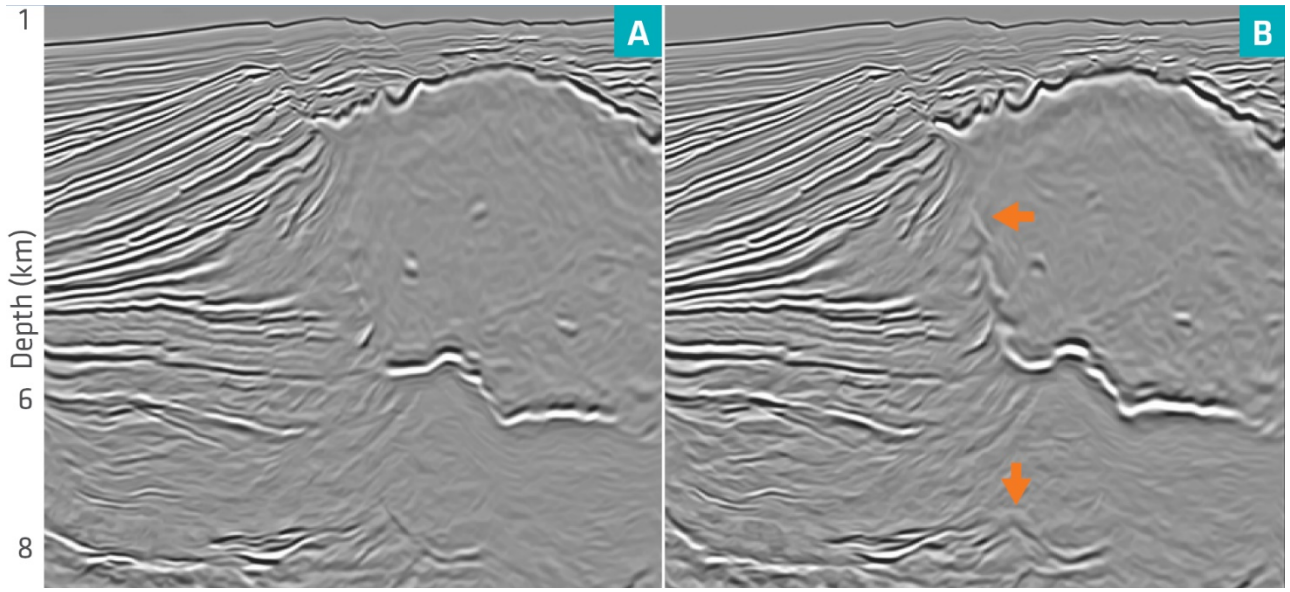

Figure 6. RTM images comparison: initial velocity model (A), vs. FWI velocity model (B). Note how the FWI velocity model improves the imaging of the salt boundaries and the sediment truncations (orange arrows).

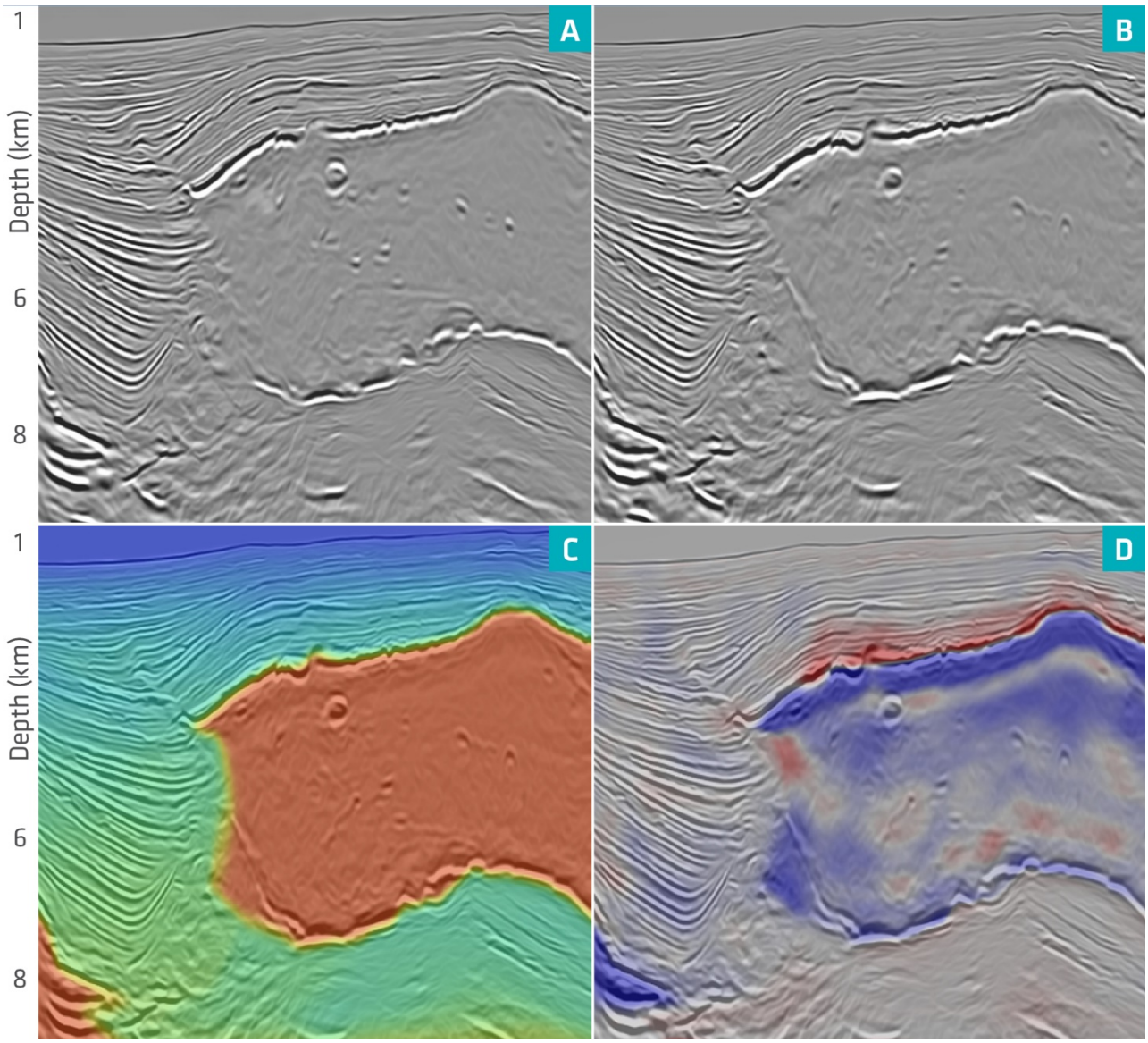

Figure 7. Comparison of RTM images using legacy (A) and FWI (B) velocity models; legacy velocity model overlaid on the FWI RTM image (C); and FWI velocity model update overlaid on the same FWI RTM image (D). Note how FWI corrects the salt interpretation by 'removing' salt (blue update) and 'adding' salt (red update) as needed.